American Mineralogist, Volume 61, pages 1241–1248, 1976

The crystal structure of bermanite, a hydrated manganese phosphate

ANTHONY R. KAMPF AND PAUL B. MOORE

Department of the Geophysical Sciences
The University of Chicago
Chicago, Illinois 60637

Abstract

Bermanite, $Mn^{2+}(H_2O)_4[Mn_2^{3+}(OH)_2(PO_4)_2]$, a 5.446(3), b 19.25(1), c 5.428(3)Å, β 110.29(4)°, monoclinic, space group $P2_1$, $Z = 2$, is a novel structure type based on dense-packed $[Mn_2^{3+}(OH)_2(PO_4)_2]^{2-}$ slabs parallel to the {010} plane linked by tetrahedral corner-sharing to insular *trans*-$[Mn^{2+}(Op)_2(H_2O)_4]$ octahedra. Chains of edge-sharing Mn^{3+}–O octahedra, expressed as $^1_\infty[Mn^{3+}(OH)(Op)_3]$, run parallel to the [101] direction and are corner-linked by the (PO_4) tetrahedra to form the slabs. A compact slab approximates local $[C \cdot A \cdot B \cdot C]$ anion packing where the A and B layers are fully occupied and the C layers only one-quarter occupied.

$R(hkl) = 0.059$ for 1254 independent reflections. The average interatomic distances are $Mn^{3+}(1)$–O 2.020Å, $Mn^{3+}(2)$–O 2.023Å, $Mn^{2+}(3)$–O 2.186Å, P(1)–O 1.550Å and P(2)–O 1.548Å. Local dense-packing and pseudo-orthogonal character of the structure allow several kinds of twinning, which are explicable on the basis of local structure geometry.

Introduction

Bermanite occurs in moderate abundance at several pegmatites (Moore, 1973) as a late-stage hydrothermally reworked product of primary manganese–iron phosphates, in particular triplite, $(Mn,Fe)_2^{2+}(F,OH)(PO_4)$. Originally described by Hurlbut (1936) from a pegmatite on the 7-U-7 Ranch, west of Hillside, Bagdad district, Arizona, it occurred in veinlets and cavities which cut and line triplite. Hurlbut established orthorhombic holosymmetry from single-crystal goniometric and X-ray study which afforded $a = 6.25$Å, $b = 8.92$Å, $c = 19.61$Å, and he proposed the composition $(Mn,Mg)_5^{2+}(Mn,Fe)_8^{3+}(PO_4)_8(OH)_{10} \cdot 15H_2O$ based on the analysis of F. A. Gonyer. A space group was not proposed. Leavens (1967), upon reexamining bermanite from the type locality as well as from other hitherto unrecorded locations, confirmed the orthorhombic symmetry and determined the cell constants $a = 6.20$Å, $b = 8.92$Å, $c = 19.20$Å with space group $C222_1$. From space-group restrictions and an electron microprobe analysis, he proposed the ideal formula $Mn^{2+}Mn_2^{3+}(PO_4)_2(OH)_2 \cdot 4H_2O$, $Z = 4$. Hurlbut and Aristarain (1968) studied bermanite from the triplite-bearing El Criollo pegmatite near Córdoba, Argentina, and detected persistent twinning which they subsequently confirmed from restudy of the type material. The twin laws observed as well as non-orthorhombic orientation of the optical indicatrix forced them to conclude that bermanite is sensibly monoclinic with the cell constants $a = c = 5.426$Å, $b = 19.206$Å, $\beta = 110°30'$ (on crystals from Argentina) and the space group $P2_1$. A new analysis of bermanite from the type locality confirmed the ideal formula proposed by Leavens with $Z = 2$.

Recently, Mr. J. E. Johnson of the South Australian Museum sent us several specimens of bermanite crystals from the McMahon pegmatite near Olary, South Australia. The mineral replaces triplite along fracture surfaces and occurs in association with phosphosiderite, strengite, siderite, hureaulite, rockbridgeite, manganese oxides, and an unknown yellow fibrous mineral. The bermanite crystals are of exceptional quality and up to 1 mm in maximum dimension. Twinning is prevalent; however, a small untwinned individual, eminently suitable for crystal structure analysis, was recovered with little difficulty. Knowledge of the crystal structure would establish the true symmetry and ideal chemical formula of bermanite and would explain the various twin laws determined by Hurlbut and Aristarain.

Our principal motivation for determining crystal

structures of aquated transition-metal phosphates, of which bermanite is a member, is to establish the nature of polyhedral clustering of the octahedra and to define a sharp link between these structures and their paragenetic settings. Bermanite is of particular interest because it is one of the few mineral species which contains essential Mn^{3+}, an ion expected to evince pronounced Jahn-Teller tetragonal distortion in an octahedral oxygen environment for the high-spin d^4 state. The similarity between the formulae of bermanite and whitmoreite, $Fe^{2+}(H_2O)_4[Fe_2^{3+}(OH)_2(PO_4)_2]$, adds interest to the species, although the two are in no way isotypic. We suspected that Jahn-Teller distortion and the subsequent severe anisotropy in electron density about Mn^{3+} compared with spherically symmetric Fe^{3+} may furnish an arrangement of octahedra quite distinct from that found in whitmoreite.

Experimental

A crystal of bermanite, prismatic parallel to the *a* axis and averaging 0.07 mm in thickness and 0.18 mm in length was selected for study. Precession and Weissenberg photographs showed the crystal to be untwinned. Monoclinic symmetry was suggested by a small inequality in the *a*- and *c*-crystallographic axes and by the intensities of the diffraction spots. The crystal was mounted parallel to the *a* axis, and data were collected on an automated four-circle diffractometer, utilizing graphite monochromatized Mo$K\alpha$ radiation, $2\theta_{max} = 55°$, scan speed 2° min^{-1}, with 20 second stationary background measurements on each side of the peak. A total of 2697 reflections were recorded. Since a relatively wide peak scan was necessary for our crystal and since the reflections along b^* are closely spaced, significant overlap was encountered for many strong reflections and this was attested by asymmetric background counts. These reflections were eliminated from further data reduction. In all, 273 reflections were rejected, and in every case but one (1.21.0) their symmetry equivalent reflection was recovered and preserved for data reduction. Twenty-six additional reflections were eliminated by space-group extinction. Absorption correction was not applied owing to the relatively low linear absorption coefficient ($\mu = 40.0$ cm^{-1}), the small size of the crystal and its approximately cylindrical shape. Reduction of the raw data to obtain $|F_o|$ was achieved through averaging symmetry equivalent reflections and accepting only those whose backgrounds were symmetrical. After correction for Lorentz and polarization effects, 1254 independent $|F_o|$ remained for the ensuing structure analysis. Errors assigned to the reflections followed the procedure adopted by Moore and Araki (1976). Least-squares refinement of 30 reference reflections established the cell criteria.

Solution and refinement of the structure

Despite the relatively simple composition for bermanite, strong homometric character was encountered, and the structure determination was not a trivial task. The three-dimensional Patterson synthesis, $P(uvw)$, revealed several pairs of vectors (**u,v,w**; ½−**u,v**,½−**w**) and a prominent vector at (½,0,½). Such relationships are not inherent in the space groups $P2_1$ or $P2_1/m$, and we concluded that a pronounced substructure relation prevailed for atoms in independent positions. The vector pairs and the vector at (½,0,½) were judged to result from two nonequivalent manganese atoms, Mn(1) and Mn(2), in general positions which were related to each other by (x,y,z) of Mn(1)–(x,y,z) of Mn(2) = (½,0,½) for the space group $P2_1$. All vectors between equivalent atoms are given by $2x$, ½, $2z$. Thus, the Mn(1)–Mn(1)′ and Mn(2)–Mn(2)′ vectors almost exactly overlap owing to their pseudo-symmetric relationship to each other. The Mn(3), $P(1)$ and $P(2)$ positions were established through a search of the vectors remaining in $P(uvw)$. Trial positions were submitted to a β-general synthesis, described by Ramachandran and Srinivasan (1970). Although the oxygen atoms associated with the phosphate tetrahedra and the OH^- groups were clearly resolved, the coordination about Mn(3) was puzzling and resisted easy interpretation. It was then discovered that Mn(3) exhibited a pseudo-symmetric relationship and a choice of one of three possible positions was required; a split residual peak proved to be the correct position. Redefining Mn(3) resulted in unambiguous location of all non-hydrogen atoms. A trial bond-distance calculation proved in good agreement with anticipated Mn^{2+}–O, Mn^{3+}–O and P^{5+}–O distances.

Despite the pronounced homometric character of the structure, refinement of the atomic coordinates and isotropic thermal vibration parameters proceeded without difficulty. We employed a highly modified version of the familiar ORFLS program of Busing *et al.* (1962), scattering curves for Mn^{2+}, Mn^{3+}, P^{3+}, and O^{2-} from Cromer and Mann (1968) and anomalous dispersion corrections for the cations (Cromer and Liberman, 1970). Five cycles of full-matrix scale factor, atomic parameters and isotropic thermal vibration parameter refinement converged to

$R = 0.059$ and $R_w = 0.065$, where $R = \Sigma||F_o| - |F_c||/\Sigma|F_o|$ and $R_w = [\Sigma_w(|F_o| - |F_c|)^2/\Sigma_w F_o^2]^{1/2}$ for all 1254 $|F_o|$. The final cycle minimized $\Sigma_w||F_o| - |F_c||^2$ where $w = \sigma_F^{-2}$. The "goodness of fit," $S = \Sigma_w||F_o| - |F_c||^2/(n - m)$ where n = number of independent F_o and m = number of parameters is 4.06. The scale factor, s, refined to 1.016(3). Atomic coordinates and isotropic thermal vibration parameters are presented in Table 1, and the structure factors are listed in Table 2.[1]

TABLE 1. Bermanite: atomic coordinates and isotropic thermal vibration parameters

Atom	x	y	z	β(Å²)
Mn(1)	0.4250(4)	0.0000	0.2368(4)	0.53(3)
Mn(2)	.9207(4)	.0013(2)	.7361(4)	0.55(3)
Mn(3)	.5386(5)	.2509(2)	.5082(5)	1.58(4)
P(1)	.4450(6)	.0958(3)	.7116(7)	0.53(6)
P(2)	.3951(6)	.9046(2)	.7603(6)	0.44(6)
O(1)	.327(2)	.0749(5)	.415(2)	0.9(2)
O(2)	.514(2)	.9255(5)	.057(2)	0.6(1)
O(3)	.292(2)	.0605(5)	.870(2)	0.7(2)
O(4)	.549(2)	.9398(5)	.605(2)	0.7(2)
O(5)	.739(2)	.0743(5)	.829(2)	0.8(2)
O(6)	.101(2)	.9260(5)	.644(2)	0.6(2)
O(7)	.409(2)	.1742(6)	.726(2)	0.9(2)
O(8)	.597(2)	.3254(7)	.257(2)	0.9(2)
OH(1)	.786(2)	.0344(5)	.377(2)	0.8(2)
OH(2)	.059(2)	.9713(5)	.101(2)	0.5(1)
OW(1)	.838(2)	.1863(6)	.443(2)	1.7(2)
OW(2)	.241(2)	.3156(6)	.599(2)	1.6(2)
OW(3)	.255(2)	.2042(6)	.133(2)	1.4(2)
OW(4)	.821(2)	.2909(6)	.877(2)	1.8(2)

[1] To obtain a copy of Table 2, order Document AM-76-030 from the Business Office, Mineralogical Society of America, 1909 K Street, N.W., Washington, D.C. 20006. Please remit $1.00 in advance for the microfiche.

Description of the structure

The structure of bermanite is based on linear edge-sharing chains of Mn^{3+}–O octahedra which run parallel to the [101] direction. Each shared edge is linked by one phosphate oxygen (Op) and one hydroxyl group (OH) and the remaining vertices receive Op. Thus, the chain formula can be expressed as $^1_\infty[Mn^{3+}(OH)(Op)_3]$. The phosphate tetrahedra link in such a way to form a dense-packed slab parallel to {010} with formal composition $[Mn^{3+}_2(OH)_2(PO_4)_2]^{2-}$. This compact slab is based on a local $[C \cdot A \cdot B \cdot C]$ packing where the A and B layers are fully occupied and the C layers are only one quarter occupied. The C layers, which correspond to the terminal Op pointing away from the slabs, link to the insular Mn^{2+}–O octahedra which bridge slabs sepa-

TABLE 3. Bermanite: interatomic distances

Mn(1)		Mn(2)		Mn(3)		P(1)		P(2)	
Mn(1)- O(2)	1.892	Mn(2)- O(5)	1.887	Mn(3)- O(8)	2.079	P(1)-O(7)	1.528	P(2)-O(8)	1.528
- O(1)	1.914	- O(6)	1.912	- O(7)	2.160	-O(3)	1.549	-O(4)	1.536
-OH(2)	1.949	-OH(1)	1.939	-OW(1)	2.177	-O(5)	1.558	-O(6)	1.560
-OH(1)	1.960	-OH(2)	1.949	-OW(4)	2.196	-O(1)	1.563	-O(2)	1.566
- O(3)	2.200	- O(3)	2.211	-OW(2)	2.231	average	1.550	average	1.548
- O(4)	2.203	- O(4)	2.239	-OW(3)	2.271				
average	2.020	average	2.023	average	2.186				
						O(3)-O(7)	2.48	O(6)-O(8)	2.48
						O(1)-O(7)	2.49	O(2)-O(8)	2.50
O(3)-OH(2)	2.69	O(5)-OH(1)	2.67	O(7)-OW(2)	2.88	O(3)-O(5)	2.53	O(4)-O(6)	2.53
O(1)-OH(1)	2.69	O(3)-OH(2)	2.69	O(8)-OW(3)	2.92	O(1)-O(3)	2.56	O(4)-O(8)	2.54
O(1)-OH(2)	2.70	O(6)-OH(2)	2.71	O(8)-OW(1)	3.00	O(5)-O(7)	2.56	O(2)-O(4)	2.54
O(2)-OH(2)	2.72	O(5)-OH(2)	2.72	OW(2)-OW(4)	3.03	O(1)-O(5)	2.56	O(2)-O(6)	2.57
O(4)-OH(1)	2.76	O(4)-OH(1)	2.76	OW(1)-OW(3)	3.06	average	2.53	average	2.53
O(2)-OH(1)	2.79	O(6)-OH(1)	2.77	O(7)-OW(4)	3.08				
O(2)- O(3)	2.90	O(4)- O(5)	2.89	O(7)-OW(3)	3.09				
O(1)- O(4)	2.90	O(3)- O(6)	2.90	O(8)-OW(2)	3.12				
O(1)- O(3)	2.91	O(4)- O(6)	2.95	OW(1)-OW(4)	3.13				
O(2)- O(4)	2.93	O(3)- O(5)	2.95	O(7)-OW(1)	3.22				
O(4)-OH(2)	3.14	O(3)-OH(1)	3.15	O(8)-OW(4)	3.23				
O(3)-OH(1)	3.15	O(4)-OH(2)	3.19	OW(2)-OW(3)	3.34				
average	2.86	average	2.86	average	3.09				

Standard errors: Mn-O, P-O ± 0.009 – 0.013Å; O-O′± 0.010 – 0.019Å

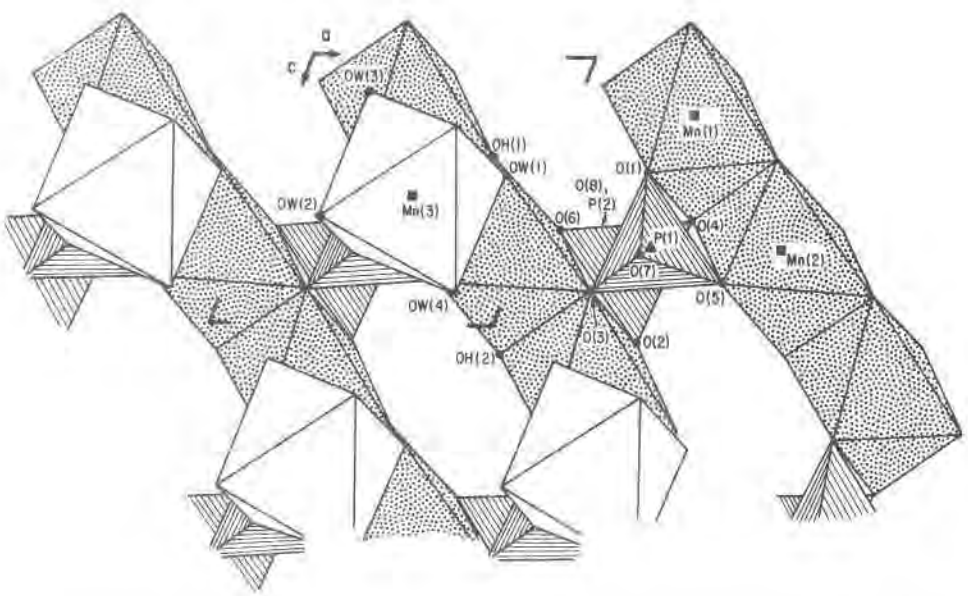

FIG. 1. Polyhedral diagram of the bermanite structure down [010]. The Mn^{3+}–O octahedra are stippled, the Mn^{2+}–O octahedra unshaded, and the P–O tetrahedra are ruled. The bridging Mn^{2+}–O octahedron above the $[Mn_2^{3+}(OH)_2(PO_4)_2]^{2-}$ sheets are linked via two tetrahedral vertices, the remaining four octahedrally coordinating ligands consisting of water molecules.

rated by $b/2$. The Mn^{2+}–O octahedron is further ligated by four water molecules and can, therefore, be written *trans*-$[Mn^{2+}(Op)_2(H_2O)_4]$. The dense slabs parallel to {010} with relatively few bonds between them is consistent with the perfect cleavage parallel to {010}. With the structural information at hand, we propose to write the bermanite formula as $Mn^{2+}(H_2O)_4[Mn_2^{3+}(OH)_2(PO_4)_2]$, which expresses the compact region of the structure. Figure 1 shows a fragment of one such slab viewed down the b axis with the bridging Mn^{2+}–O octahedron above it. Figure 2 is a view down $[10\bar{1}]$showing the linkage between adjacent slabs, and Figure 3 is an idealized sketch of the close-packed slab. It is seen that the a- and c-crystallographic axes are each the sum of one octahedral plus one tetrahedral edge. Although the

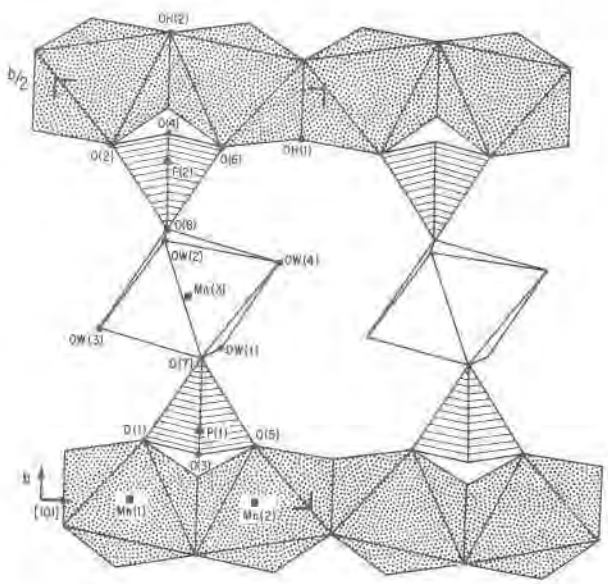

FIG. 2. A view of the bermanite structure down the $[10\bar{1}]$ axis Note the role of the bridging Mn^{2+}–O octahedron

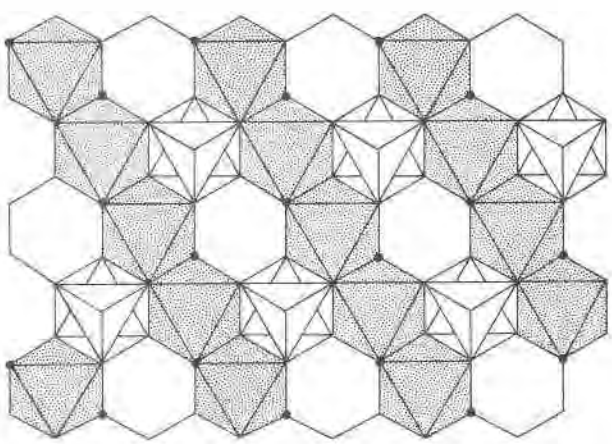

FIG. 3. The bermanite $[Mn_2^{3+}(OH)_2(PO_4)_2]^{2-}$ sheet idealized according to close-packing. Note the pronounced pseudo-hexagonal character. The $(OH)^-$ ligands are represented as solid disks.

ideal β-angle would be 120°, Jahn-Teller distortion, discussed further on, reduces this to 110.3°.

Bermanite is yet another example where insular Me^{2+}–O octahedra bridge dense, compact Me^{3+}–O + P^{5+}–O sheets in phosphate minerals. Other examples include the laueite group, $Mn^{2+}(H_2O)_4[Fe_2^{3+}(OH)_2(H_2O)_2(PO_4)_2]\cdot 2H_2O$ (Moore, 1975), and whitmoreite, $Fe^{2+}(H_2O)_4[Fe_2^{3+}(OH)_2(PO_4)_2]$ (Moore *et al.*, 1974). This pattern will aid in interpretation of as yet unknown structures, but in addition it emphasizes the tendency for Me^{3+}–O octahedra to densely cluster with PO_4 tetrahedra in coexistence with insular Me^{2+}–O species. This point is of considerable importance toward unravelling the complex parageneses of coexisting transition-metal phosphates, and suggests that insular divalent octahedral species may coexist in the fluid with more complex clusters of trivalent octahedral species in late-stage assemblages.

Polyhedral interatomic distances

Both Mn^{3+}–O octahedra are elongated (Table 3). Mn(1) has two oxygens in *trans*-configuration at an average distance of 2.20Å with four planar oxygens at an average distance of 1.93Å. Mn(2) has two at an average of 2.23Å and four at an average of 1.92Å. This 4 + 2 coordination is typical of transition-metal ions with d^4 or d^9 high-spin configurations, since their electron clouds are subjected to pronounced Jahn-Teller distortion in octahedral fields. Shannon *et al.* (1975) found that the average Mn^{3+}–O distances for Jahn-Teller distorted octahedra increase in a predictable fashion with the degree of distortion. The average distances of Mn(1)–O and Mn(2)–O calculated from their equation are 2.02 and 2.03Å respectively, which closely corresponds to the 2.02Å average observed for Mn(1)–O and Mn(2)–O in bermanite.

Hydrogen bonds

The locations of possible hydrogen bonds were inferred from geometrical and electrostatic valence balance arguments. The potential donors of hydrogen bonds are OH(1), OH(2), OW(1), OW(2), OW(3) and OW(4). We propose the following hydrogen bonds: OW(1)···OH(1), 2.95Å; OW(1)···O(7), 2.96Å; OW(2)···O(2), 2.83Å; OW(2)···O(6), 2.83Å; OW(3)···O(1), 2.88Å; OW(3)···O(7), 2.68Å; OW(4)···O(8), 2.82Å; OW(4)···OW(3), 2.83Å; OH(1)···OH(2), 2.73Å. The angles O–OW–O′ compute to OH(1)–OW(1)–O(7) 91.4°; O(2)–OW(2)–O(6) 80.2°; O(1)–OW(3)–O(7) 103.1°; and O(8)–OW(4)–OW(3) 106.1°. According to this model, O(1), O(2), O(6), O(8), OH(1), OH(2), and OW(3) each receives one hydrogen bond and O(7) receives two.

This is not the only reasonable hydrogen bonding model based on geometrical arguments; however, it is the one which yields the best fit between electrostatic valence balance and variations in individual bond distances, as discussed in the next section.

Discussion

Electrostatic valence balance

The principle of electroneutrality has become one of our more important interpretive tools in crystal structure analysis. In its simplest form, we are provided with a means of discriminating oxo-anions, hydroxyl groups and water molecules when the struc-

TABLE 4. Bermanite: electrostatic bond strengths (po) and their sums about the anions

Anion	Mn(1)	Mn(2)	Mn(3)	P(1)	P(2)	H(d)	H(a)	Σpo
O(1)	3/6(7/12)			5/4			1/6	1.92(2.00)
O(2)	3/6(7/12)				5/4		1/6	1.92(2.00)
O(3)	3/6(4/12)	3/6(4/12)		5/4				2.25(1.92)
O(4)	3/6(4/12)	3/6(4/12)			5/4			2.25(1.92)
O(5)		3/6(7/12)		5/4				1.75(1.82)
O(6)		3/6(7/12)			5/4		1/6	1.92(2.00)
O(7)			2/6	5/4			2/6	1.92
O(8)			2/6		5/4		1/6	1.75
OH(1)	3/6(7/12)	3/6(7/12)				5/6	1/6	2.00(2.17)
OH(2)	3/6(7/12)	3/6(7/12)				5/6	1/6	2.00(2.17)
OW(1)			2/6			10/6		2.00
OW(2)			2/6			10/6		2.00
OW(3)			2/6			10/6	1/6	2.17
OW(4)			2/6			10/6		2.00

ture determination does not provide resolution of the hydrogen atom locations.

Table 4 lists the valence bond strengths for the oxygen atoms in bermanite on the basis of the number and kinds of cations coordinating to them. Included are the hydrogen bonds proposed earlier. A bond strength of $s = 5/6$ is ascribed to a hydrogen donor (H*d*) and $s = 1/6$ for a hydrogen acceptor (H*a*) as suggested by Baur (1970) on empirical grounds. The electrostatic bond-strength sums all fall within the acceptable range for a stable crystal structure.

Baur (1970) correlated the variations in the sums of bond strengths, p_0, received by anions to their individual distances to coordinated cations. Oversaturated oxygen atoms, that is, those which receive bond-strength sums from cations in excess of 2.00, generally show longer metal-oxygen distances, while shorter than average distances are found for undersaturated oxygens. This correlation is borne out by the Mn^{3+}–O and Mn^{2+}–O distances in bermanite as illustrated in Table 5. It should be noted, however, that ambiguities in assignment of hydrogen bonds were resolved in favor of this correlation.

The question arises as to the origin of the elongation in the Mn^{3+}–O octahedra. Is it the result of the oversaturation of two *trans* oxygens or is it the result of the Jahn-Teller distortion? Moore and Araki (1974) emphasized the ordering of Mn^{3+} in the crystal structure of pinakiolite, $Mg_2Mn^{3+}O_2[BO_3]$, which was consistent with electrostatically oversaturated anions distributed at an opposing octahedral apical pair and undersaturated anions distributed about the remaining four meridional apices. This argument leads to the hypothesis that stable structures involving octahedral Mn^{3+} in mineral oxide crystals are those whose *trans* oxygens are oversaturated and whose meridional oxygens are undersaturated *if an isotropic M^{3+} cation is placed in that site.* Thus, proceeding from idealized structure types, those fulfilling this criterion will be likely candidates for Mn^{3+} oxysalts. Although spherically symmetrical cations like Al^{3+} and Fe^{3+} form isomorphic salts for a large number of structure types, Mn^{3+} substitution is probably limited only to those which fulfill the criteria of *trans*-oxygen oversaturation and meridional oxygen undersaturation. Since structural isomorphism between Mn^{3+} and Al^{3+} and Fe^{3+} appears limited in oxysalt chemistry, we favor the Jahn-Teller distortion itself as the basis for the selection of those structure types where Mn^{3+} will be stable in an octahedral field.

This suggests that bond strengths should be redistributed in an unsymmetrical field as induced by Mn^{3+} so that the assignments are less for the two longer bonds and greater for the four shorter bonds. Confirmation of this view is seen in the poor correlation between the bond strength with the P–O bond distances and the obvious improvement in this correlation with the suggested redistribution. We propose an addition of $\Delta s = +1/12$ to be applied to each of the four short meridional bonds and a subtraction of $\Delta s = -2/12$ from the bond strengths of the longer apical bonds and recommend $s = 7/12$ for meridional

TABLE 5. Bermanite: variation in Me–O distances (δd) compared to variation in electrostatic bond strength sums of the anions ($\delta\Sigma_{po}$)

	Mn(1)		Mn(2)		Mn(3)		P(1) or P(2)	
Anion	δd	$\delta\Sigma p_o$	δd	$\delta\Sigma p_o$	δd	$\delta\Sigma p_o$	δd	$\delta\Sigma p_o$
O(1)	-.11	-.14					+.01	-.05(+.08)
O(2)	-.13	-.14					+.02	-.04(+.08)
O(3)	+.18	+.19	+.19	+.22			.00	+.28(.00)
O(4)	+.18	+.19	+.22	+.22			-.01	+.29(.00)
O(5)			-.14	-.28			+.01	-.22(+.10)
O(6)			-.11	-.11			+.01	-.04(+.08)
O(7)					-.03	-.05	-.02	-.06(.00)
O(8)					-.11	-.22	-.02	-.21(-.17)
OH(1)	-.06	-.06	-.08	-.03				
OH(2)	-.07	-.06	-.07	-.03				
OW(1)					-.01	+.03		
OW(2)					+.05	+.03		
OW(3)					+.09	+.20		
OW(4)					+.01	+.03		

bonds and $s = 4/12$ for apical bonds. Further support of these assignments comes from pinakiolite (Moore and Araki, 1974) where all four non-equivalent anions receiving apical Mn^{3+}–O bonds are oversaturated by $\Delta p_0 = +2/12$ when the isotropic model ($s = 3/6$) is adopted.

Relationship of bermanite to whitmoreite

With the substitution of Fe for Mn, the formula of bermanite becomes identical with that of whitmoreite (Moore *et al.* 1974). The gross structural features of these minerals are also rather similar. Both possess sheets of octahedra which can be ideally written $[Me^{3+}_2(OH)_2(Op)_6]$. In both instances, the (PO_4) tetrahedra share three of their four vertices with octahedra in the sheet to form a slab with formal composition $[Me^{3+}_2(OH)_2(PO_4)_2]^{2-}$. The tetrahedra point up and down away from the slab, and share their remaining oxygens with an insular Me^{2+}–O octahedron. Each Me^{2+} bonds to one tetrahedral oxygen from each of the two adjacent slabs, thereby linking slabs together; and each Me^{2+} is further coordinated by four water molecules so that the octahedral formula can be written *trans*-$[Me^{2+}(Op)_2(H_2O)_4]$. The distance between the slabs in each is similar, 9.63Å for bermanite and 9.98Å for whitmoreite.

The linkage of the octahedra in the sheets, however, differs markedly. In whitmoreite, the Fe^{3+}–O octahedra form edge-sharing dimers which further link together by sharing corners. We submit these differences as further proof for the stabilization of the bermanite structure type by Jahn-Teller distortion. An "Fe^{3+}–bermanite" or "Mn^{3+}–whitmoreite" would lead to serious deviations from electrostatic neutrality.

On structural grounds, therefore, the substitutions of Fe^{3+} and Mn^{3+} for each other in these structures is predicted to be quite limited. There is no structural reason, however, to limit to substitution of Fe^{2+} and Mn^{2+} at the insular octahedral sites. On grounds of oxidation potential, Mn^{3+} and Fe^{2+} are incompatible. As expected, Moore *et al.* (1974) note nearly equal amounts of Fe^{2+} and Mn^{2+} in whitmoreite with no evidence of Mn^{3+}, and Hurlbut and Aristarain (1968) and Leavens (1967) report small amounts of Fe^{3+}, but no Fe^{2+}, in bermanite.

Symmetry and twinning

The pseudo-orthorhombic morphology and cell geometry of bermanite is the result of an internal structure which does not deviate greatly from orthorhombic symmetry. In fact, a small shift in the slabs relative to one another with a reorientation of the insular octahedron would result in orthorhombic symmetry of the structure, even though the structural topology does not change. The reorientation of the insular octahedra would bring the water molecules in adjacent octahedra too close together, and it appears that steric restrictions are responsible for the monoclinic symmetry.

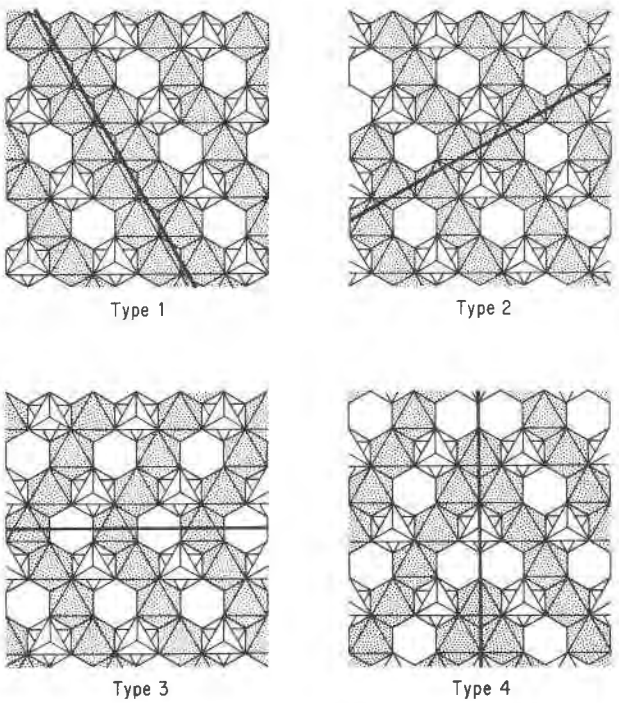

FIG. 4. Twinning schemes for bermanite down the [010] direction. The composition plane is shown bold. Composition plane and twin axis are: Type 1 {$\bar{1}$01}, [101]; Type 2, {101}, {$\bar{1}$01}; Type 3, {001}, [100]; Type 4, {$\bar{3}$01}, [100].

Twinning is the rule, rather than the exception, for bermanite. Hurlbut and Aristarain (1968) note four common types of twinning in bermanite. Specified in terms of composition plane and twin axis, these are: (1) {$\bar{1}$01}, [101]; (2) {101}, [$\bar{1}$01]; (3) {001}, [100]; (4) {$\bar{3}$01}, [100]. All of these can be explained structurally, and Figure 4 shows how the four types of twinning could occur in idealized close-packed bermanite slabs. Type 3 is the simplest and merely reverses direction of the octahedral chains. Type 4 results in a curious wedge-like arrangement reminiscent of the octahedral wedges found in the crystal structure of synadelphite, $Mn^{2+}_9(OH)_9(H_2O)_2$ $(AsO_3)(AsO_4)_2$ (Moore, 1970). Type 2 creates local arrangements similar to a sheet in hematite, and Type 1 creates an octahedral double band. Twinning on the scale of unit-cell dimensions, of course, could lead to

a novel structure type, and it is conceivable that some bermanite-like phases might exist as a result of this "chemical twinning." We suggest that bermanite of unusual development be carefully checked by single-crystal study in the possible event that a related, but distinct, structure type may exist.

Acknowledgments

We thank Mr. J. E. Johnson for the fine bermanite specimen, which concluded the years of search for a suitable single crystal. Grateful appreciation is also extended Professor C. S. Hurlbut, Jr., Professor P. Leavens and Mr. W. L. Roberts who donated samples. Dr. Takaharu Araki assisted in the various stages of the crystal structure analysis.

The National Science Foundation supported this work through the grant NSF GA 40543 and through the Materials Research Laboratory grant administered to The University of Chicago.

References

Baur, W. H. (1970) Bond length variation and distorted coordination polyhedra in inorganic crystals. *Trans. Am. Crystallogr. Assoc.* **6,** 129–155.

Busing, W. A., K. O. Martin and H. A. Levy (1962) ORFLS, a Fortran crystallographic least-squares program. *U. S. Natl. Tech. Inf. Serv.* ORNL-TM-**305.**

Cromer, D. T. and D. Liberman (1970) *Los Alamos Scientific Laboratory, Univ. of Calif. Report* **LA-4403, UC-34.**

——— and J. B. Mann (1968) X-ray scattering factors computed from numerical Hartree-Fock wave-functions. *Acta Crystallogr.* **A24,** 321–324.

Hurlbut, C. S., Jr. (1936) A new phosphate, bermanite, occurring with triplite in Arizona. *Am. Mineral.* **21,** 656–661.

——— and L. F. Aristarain (1968) Bermanite and its occurrence in Córdoba, Argentina. *Am. Mineral.* **53,** 416–431.

Leavens, P. B. (1967) Reexamination of bermanite. *Am. Mineral.* **52,** 1060–1066.

Moore, P. B. (1970) Crystal chemistry of the basic manganese arsenates: IV. Mixed arsenic valences in the crystal structure of synadelphite. *Am. Mineral.* **55,** 2023–2037.

——— (1973) Pegmatite phosphates: descriptive mineralogy and crystal chemistry. *Mineral. Rec.* **4,** 103–130.

——— (1975) Laueite, pseudolaueite, stewartite and metavauxite: a study in combinatorial polymorphism. *Neus Jahrb. Mineral. Abh.* **123,** 148–159.

——— and T. Araki (1974) Pinakiolite, warwickite and wightmanite: crystal chemistry of complex 3Å wallpaper structures. *Am. Mineral.* **59,** 985–1004.

——— and T. Araki (1976) A mixed valence solid solution series: crystal structures of phosphoferrite, $Fe_3^{2+}(H_2O)_3[PO_4]_2$; and kryzhanovskite, $Fe_3^{3+}(OH)_3[PO_4]_2$. *Inorg. Chem.* **15,** 316–321.

———, A. R. Kampf, and A. J. Irving (1974) Whitmoreite, $Fe^{2+}Fe_2^{3+}(OH)_2(H_2O)_4[PO_4]_2$, a new species: its description and atomic arrangement. *Am. Mineral.* **59,** 900–905.

Ramachandran, G. N. and R. Srinivasan (1970) *Fourier Methods in Crystallography.* Wiley-Interscience, New York, p. 96-119.

Shannon, R. D., P. S. Gumerman and J. Chenavas (1975) Effect of octahedral distortion on mean Mn^{3+}–O distances. *Am. Mineral.* **60,** 714–716.

Manuscript received, February 6, 1976; accepted for publication, July 2, 1976.